Design and Development of Automatic Magnetic Setup for Hybrid Single-Point Diamond Turning of Optical Components

Shahrokh Hatefi[1*], Khaled Abou-El-Hossein[2]
1. Ultra-High Precision Manufacturing Laboratory, Department of Mechatronics Engineering, Nelson Mandela University, Port Elizabeth, South Africa.
Email: Shahrokh.Hatefi@mandela.ac.za (Corresponding author)
2. Ultra-High Precision Manufacturing Laboratory, Department of Mechatronics Engineering, Nelson Mandela University, Port Elizabeth, South Africa.
Email: Khaled.Abou-El-Hossein@mandela.ac.za

Received: 7 September 2022 Revised: 19 October 2022 Accepted: 14 December 2022

ABSTRACT
Single-Point Diamond Turning (SPDT) has been widely used in manufacturing of optical components for critical applications including military, defense, aerospace, computer science, electronics, medical, and dental. Magnetic Field (MF) assistance is a recent non-conventional assistive technique that could be used during SPDT process to improve the machining conditions. Recent experimental studies show that using MF assisted SPDT technique can improve the optical surface roughness compared to purely mechanical SPDT process. There are a few studies conducted on the application of magnetic manipulation technique during the SPDT process. The effects of applying a strong MF during diamond cutting on the outcome of the machining process, as well as the optimum MF parameters to be used in SPDT process, are not fully discovered yet. The purpose of this research is to design and develop an automatic MF assistance system that could be used in non-conventional MF assisted and hybrid SPDT processes. The proposed automatic system is capable of communicating with the hybrid controller and precisely set/modify the desired magnetic parameters, including the generated magnetic flux density, at the cutting zone. By using the proposed system, an automatic MF assistance system in non-conventional SPDT processes could be enabled and the optimum machining conditions could be determined.

KEYWORDS: Linear Control System, Magnetic Field Assisted Machining, Non-Conventional Machining, Advanced Manufacturing, Ultra-Precision Manufacturing.

1. INTRODUCTION

Single Point Diamond Turning (SPDT) is the state-of-the-art technology for advanced manufacturing of optical components with the best possible surface finish and cutting accuracy. By using SPDT technology, manufacturing of optical components with surface roughness down to 1 nanometer is possible [1, 2]. During the ultra-high-precision SPDT process, different factors could induce the diamond tool wear and negatively affect the quality of optical surface finish. The main influencing factors are cutting temperature, cutting force, passive vibrations, material swelling/recovery, and machining parameters [3, 4]. The negative effects of influencing factors on the quality of optical surface roughness are induced when hard-to-cut materials, including titanium alloys and stainless steel, are cut. High cutting temperature, low diamond tool life, and high optical surface roughness are associated with the SPDT of hard-to-cut materials [5-7].

Different techniques have been used to reduce the effects of influencing parameters on the optical surface roughness for obtaining the best possible surface finish. By optimizing the cutting parameters and turning factors, the quality of the finished surface could be improved. Non-conventional machining techniques have been recently used during the SPDT process to improve the cutting conditions and reduce the negative effects of mentioned factors on the machining outcome. Hot machining, active-vibration, gas shielding, and Magnetic Field (MF) assistance are the techniques that have been used in non-

Paper type: Research paper
DOI: 10.30486/mjee.2023.1970273.0
How to cite this paper: Sh, Hatefi, Kh.A. El-Hossein, **"Design and Development of Automatic Magnetic Setup for Hybrid Single-Point Diamond Turning of Optical Components"**, *Majlesi Journal of Electrical Engineering*, Vol. 17, No. 2, pp. 13-21, 2023.

conventional assisted SPDT processes. Using these techniques during the SPDT process could improve the quality of optical surface finish and reduce the diamond tool wear [8-11].

One of the effective techniques that can positively impact the outcome of the SPDT process is applying a strong MFs around the cutting zone. In a normal SPDT process, Van der Waals forces and dipole-dipole interaction impact the behavior of paramagnetic particles inside the workpiece material which cause the particles attach to each other. This effect decreases the thermal conductivity of the workpiece material and increase the cutting temperature during the SPDT process. In the presence of a strong MF, the dipole moments inside the workpiece material align with the direction of MF and act as a linear chain structure, which can transfer the generated heat faster during the cutting process, while increasing the thermal conductivity of the workpiece material [12-14]. Moreover, applying a MF during the cutting process could reduce the machine tool passive vibrations. When a conductive material is rotating in the presence of a MF, eddy current is generated inside the material. The generated eddy current creates its own MF which is against the existed MF. This interaction cause reducing the kinetic energy of the vibrations while transferring it into heat energy. This effect cause reduction in the amplitude of the machine tool passive vibrations during the SPDT process [15-17].

Recently, in a few experimental studies, applying a MF around the cutting zone during the SPDT of hard-to-cut materials has shown promising results in terms of improving cutting conditions and reducing the optical surface roughness. The results of recent investigations show that applying a MF could reduce the passive vibrations and the cutting temperature during the SPDT process. However, the effects of using magnetic manipulation technique, as well as the optimum Magnetic Flux Density (MFD) for SPDT applications, are not fully understood yet. More research needs to be undertaken to determine the optimum MFD in specific SPDT processes for advanced manufacturing of engineering materials [4].

The purpose of this study is to design and develop an Automatic Magnetic Manipulation System (AMMS) for applying a MF, with controlled MFD, around the cutting zone during the SPDT process. The proposed system is capable of controlling the linear position of two strong magnets, which are placed in front of each other, at the sides of the machine's spindle, with high positioning accuracy. By using a precise control system, the distance between the magnets could be set precisely. The AMMS could help with studying the effects of applying a MF on the machining factors as well as the correlation between the applied MFD and the effects of influencing factors in SPDT of different hard-to-cut materials. By using the proposed system, the optimum MFD for SPDT of different materials could be determined. In a hybrid SPDT platform, the propose system could get connected to the hybrid controller [18, 19]. The proposed AMMS could be used in hybrid SPDT applications for applying a strong MF with controlled parameters. In the following sections, the methods used in the development of proposed AMMS are presented. Subsequently, the results of the modeling and experimental study are presented and discussed. At the end, conclusions are drawn and future works are suggested.

2. MATERIAL AND METHODS

2.1. Design of the System

The design of the system includes different mechanical and electronic components that work together as an electromechanical system to control the linear positioning of two bar magnets and precisely set the desired MFD at the cutting zone. Fig. 1 illustrates the 3D model of the designed AMMS.

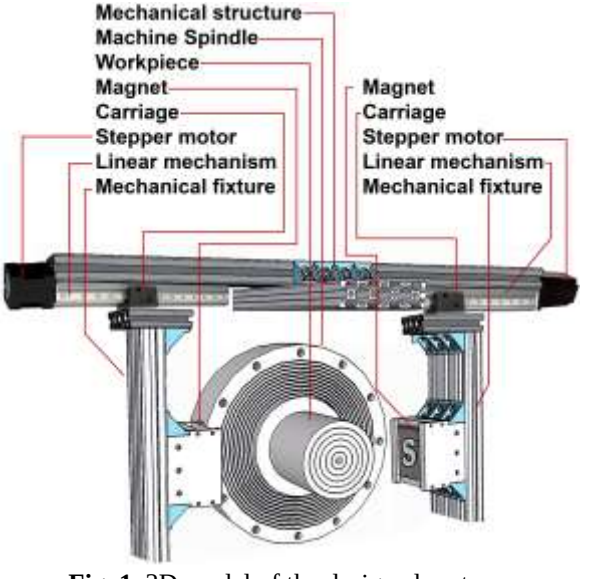

Fig. 1. 3D model of the designed system.

In the designed system, a precise control system is implemented to drive and control the linear positioning of two linear actuators, and to set the desired distance between the magnets. The system receives the desired MFD using Human-Machine Interface (HMI), and calculates the exact distance between the magnets to generate the desired MFD. A closed-loop control system, using control feedback from a hall effect sensor, is used to measure the generated MFD and to correct the positioning of the magnets real time. In a hybrid SPDT platform, the acquired data could be transmitted to the hybrid controller of the machining platform [19]. The control

system of AMMS could also receive commands from the hybrid controller and modify the desired MFD.

In the designed system, a power supply is used the provide the required energy for running the control system and the electromechanical linear mechanism. For this purpose, a S-6012 power supply, with an output voltage of 12 VDC, an output current of 5 A, and a total output power of 60 watt, is implemented within the system to supply different units, including microprocessor, motor drivers, display, and hall effect sensor. An Arduino Uno Rev3 A000066 development MCU board is implemented within the design of control system to control the performance of the mechanism and to precisely control the positioning of the bar magnets. The Arduino UNO development MCU board is based on the ATmega328P microcontroller, with 14 digital input/output pins and a clock speed of 16 MHz. The control system could calculate the desired positioning of each linear actuator and execute control signals for driving the stepper motors.

In the designed control system, for controlling the linear positioning of the linear actuators, a linear control system, Multi-Axis Automatic Controller (MAAC), is used [20, 21]. The MAAC could control the linear positioning of each actuator using closed-loop control system. The output signal of a hall effect sensor is the feedback of the system so that the generated MFD could be measured and modified. The MAAC could execute control signals for driving the stepper motor in each linear axis. The MAAC can drive the stepper motors in micro-stepping drive mode (1/32) with the maximum positioning accuracy. The generated control signals are transmitted to the stepper motor drivers. In the motor driver unit, two L298N dual full-bridge motor drivers, with specifications presented in Table 1, are used. The stepper motor drivers receive the control signals, the activation sequences of the stepper motor phase, and activate the stepper motor phases according to the transmitted control signals. This configuration enables driving the stepper motor with controlled shaft position and speed.

Two NEMA 17 hybrid stepper motors used in the linear mechanism to control the linear positioning of the bar magnets in two independent linear axis. The specifications of the NEMA 17 hybrid stepper motor are presented in Table 2. The stepper motor drivers could drive the stepper motors and control the angular position of the stepper motor's shaft. Two linear actuators are used in the proposed AMMS. The stepper motors' shaft is connected to the lead screw of the linear actuator. Therefore, in each linear mechanism, the linear positioning of the carriage could be precisely controlled. A mechanical fixture is fixed to the carriage of the linear mechanisms to fix the magnets to the carriage at the desired position. Different types of magnets can be fixed to the AMMS, and the linear distance between them could be precisely set.

Two similar linear mechanism are used in the designed system, for moving two magnets in a linear vector. In the linear actuator, a high precision, heavy load resistance SFU1605 ball-screw, with a diameter of 16 mm, a length of 200 mm, and 5 mm pitch of screw, and an effective stroke of 130 mm, is used. By using the specifications of the hybrid stepper motor, stepper motor driving mode, and the linear mechanism, the linear positioning of the system can be calculated. The NEMA 17 hybrid stepper motor has a step angle of 1.8 degree. Also, the control system could drive the hybrid stepper motors in micro-stepping drive mode with a maximum micro-step resolution of 1/32. Therefore, the maximum linear positioning of the system is 7.5 µm/step.

Table 1. Specifications of the L298N dual full-bridge motor driver

Chip	L298N
Minimum operating voltage	8 VDC
Maximum operating voltage	46 VDC
Drive current per channel	2 A
Maximum output current	4 A
Minimum logic voltage	4.5 VDC
Maximum logic voltage	7 VDC
Logic current	0-36 mA
Maximum power	25 W
Size	43*43*26 mm
Weight	26 g

Table 2. Specifications of the NEMA 17 hybrid stepper motor

Rated voltage	4 VDC
Current	1.2 A at 4 VDC
Step angle	1.8 degree
No. of phases	4
Resistance per phase	3.3 Ω
Inductance per phase	2.8 mH
Insulation resistance	100 MΩ
Holding torque	3.17 kg.cm
Detent torque	200 g.cm
Unipolar holding torque	22.2 oz-in
Rotor inertia	68 g.cm^2
Max. radial force	28 N
Max. axial force	10 N

Motor length	40 mm
Steps per revolution	200
Operating temperature	-10 to 40 °C
Temperature rise	80 °C Max
Weight	0.33 kg

Fig. 2 presents the detailed design of the control system. As illustrated in this figure, by using the HMI unit of the system, including a keypad and LCD, the desired MFD between the magnets could be set. Alternatively, in a hybrid SPDT platform, the control system could be connected to a hybrid control unit [19] and receive the data containing the desired MFD from the hybrid controller. By using the desired MFD and the specification of the implemented magnets, the control system calculates the exact linear position of each magnet. Subsequently, the control system sends the control signals to the L298N motor drivers for driving the stepper motors and moving the carriage of the linear mechanism to the desired position. A limit switch is used in each linear mechanism to define the zero position of the linear system. Moreover, a hall effect module, with analog output, is used within the control
system for measuring the generated MFD. The analog output of the hall effect sensor, is connected to the Analog to Digital (ADC) unit of the microcontroller, for measuring the existed MFD. The measured MFD is used as control feedback for setting and correcting the linear distance between the magnets to achieve the exact amount of the desired MFD at the cutting zone. In a hybrid SPDT process, the designed AMMS is capable of communicating with the hybrid controller real-time and transmit the measured MFD to the hybrid controller for further analysis by using NRF24L01wireless module.

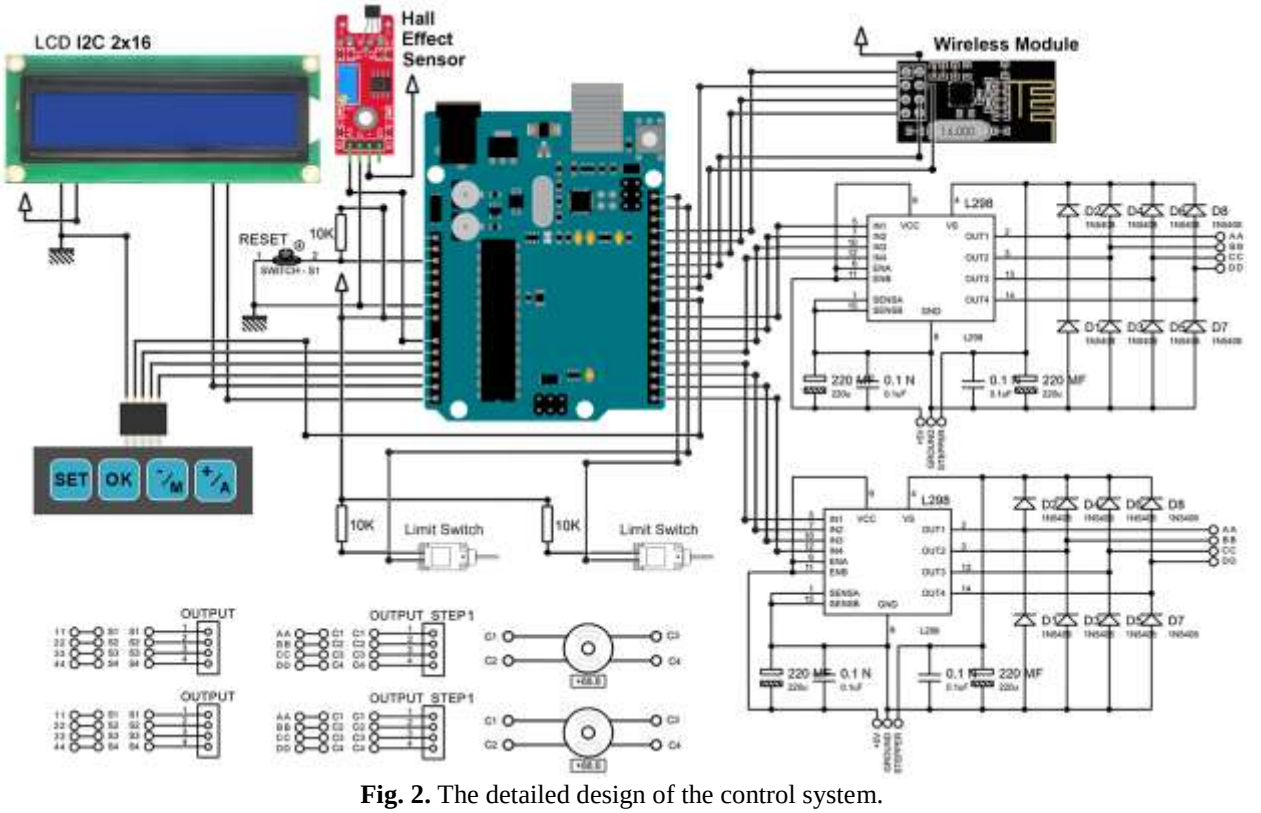

Fig. 2. The detailed design of the control system.

2.2. Magnetic Field Generation

Fig. 3 illustrates the generated MF at the cutting zone during the SPDT process. In the designed system two MRERE673 Rare Earth Rectangle 50x50x25 mm magnet are used. The magnets are fixed to the mechanical structure in front of each other. The N pole of the magnet fixed to the left linear actuator faces the S pole of the magnet that is fixed to the right linear actuator. Each magnet creates a MF with a MFD that could be calculated and measured. The maximum MFD could be generated at the center of the direct linear distance between the magnets. In this condition, the average generated MFD by each magnet could be calculated using the following equation [22]:

$$B = \frac{B_r}{\pi}\left(arctan\left(\frac{L.W}{2X\sqrt{4x1^2+L^2+W^2}}\right) - arctan\left(\frac{L.W}{2(D+X)\sqrt{4(D+X)^2+L^2+W^2}}\right)\right) \quad (1)$$

where, X is the desired distance from the magnet, Br is the magnetic remanence of magnet, L, D, and W are the dimensions of magnet. B is the magnetic flux density created by magnet at distance X, and B is the average magnetic flux density at location X. The control unit could calculate the strength of generated MFD by each magnet using Eq (1). In this condition, the average magnetic flux density at the cutting zone could be calculated using the following equation:

$$B = B_1 + B_2 \quad (2)$$

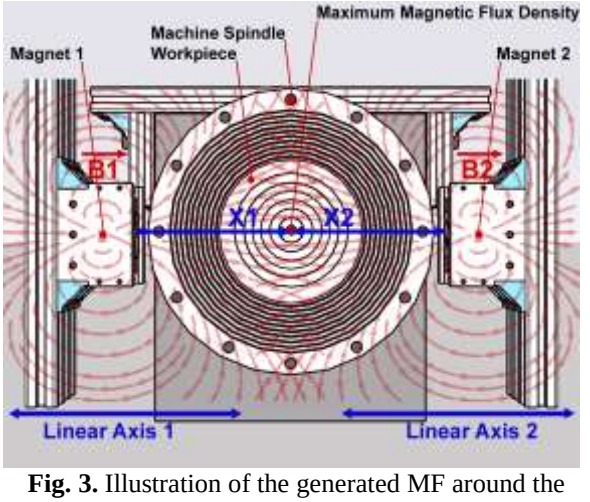

Fig. 3. Illustration of the generated MF around the cutting zone.

2.3. Modeling of Control System

After the design of the AMMS, the control system of the device has been modeled. For the modeling of the control system, MATLAB/SIMULINK software was used. Fig. 4 illustrates the overall modeling of the control system in the MATLAB/SIMULINK software. In the designed model, current and voltage subsystems are designed for simulating the performance of the hybrid stepper motor using the designed control system. Also, position and speed subsystems are used for modeling the stepper motor's shaft position and speed. The designed control system could drive the stepper motors in micro-stepping drive mode. The micro-stepping drive mode has more stability and positioning accuracy compared to other driving methods. In the modeling of the system, the mathematical equations of the hybrid stepper motor, including the differential equations, are used. These equations are given below [23]:

$$\frac{dia}{dt} = \frac{va+km.\omega.sin(N.\theta)-Ria}{L} \quad (3)$$

$$\frac{dib}{dt} = \frac{vb+Km.\omega.cos(N.\theta)-Ria}{L} \quad (4)$$

$$\frac{d\omega}{dt} = \frac{Km.ib.cos(N.\theta)-T-Km.ia.sin(N.\theta)-Kv.\omega}{J} \quad (5)$$

$$\frac{d\theta}{dt} = \omega \quad (6)$$

where, ia is the current of phase A, ib is current of phase B, va is the voltage of phase A, and vb is the voltage of phase B of the stepper motor. ω is the rotational speed of the rotor (rad/s), θ is the angular position of the rotor (rad), and T is the load torque of the stepper motor (N.m.). Other parameters are neglected in the modeling of the hybrid stepper motor. Eq (1) and Eq (2) are used in the modeling of voltage and current subsystems. Eq (3) and Eq (4) are used in designing the speed and position subsystems.

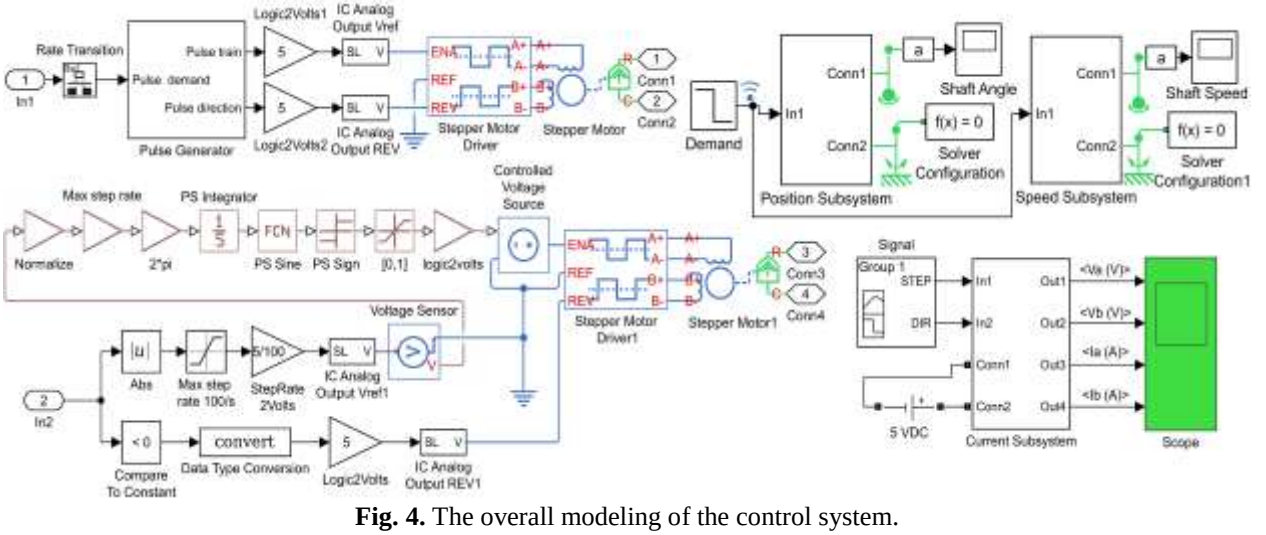

Fig. 4. The overall modeling of the control system.

2.4. Experimental Setup

After the design and modeling of the AMMS, the system was prototyped. Fig. 5 illustrates the first prototype of the AMMS. Subsequent to the design and development of the AMMS, an experimental study was performed to evaluate the positioning accuracy of the linear system, as well as the performance of the control system in controlling the positioning of the linear mechanism and driving the stepper motors with desired working parameters. In the first phase of the experimental study, different distances between the magnets were set using the HMI unit. Afterwards, the system was run while the control system was driving the stepper motors of the linear mechanisms while setting the desired linear position of each magnet. The conditions of this experimental test are presented in Table3.

The control system could theoretically calculate the generated MFD using Eq (1), Eq. (2), and the specifications of the magnets used. However, different factors could influence the generated MFD during the machining process and there is a need of feedback on the generated MFD is a specific strength of MF is desired. Therefore, a hall effect sensor is used for in-process measurement of generated MFD and to precisely set the desired strength of the MFD.

Fig. 5. The developed AMMS.

3. RESULTS AND DISCUSSION

After the design and development of the AMMS, modeling of the control system as well as experimental verifications were performed to evaluate the performance of the AMMS and justify its functionality in generating the desired MFD and measuring it. For the simulations of the control system, MATLAB/SIMULINK software was used. The results show that the designed control system is capable of driving the hybrid stepper motor in micro-stepping drive mode ith high precision. After the modeling of the control system, the simulation was run for 0.1 second. The results of the simulation include the phase voltage, the phase current, the rotor speed, and the rotor position of the stepper motor. Fig. 6 presents the generated waveforms after running the simulation.

In the generated waveforms, V_{ph} illustrates the phase voltage of the stepper motor. V_1 presents the phase voltage of phase A and V_2 presents the phase voltage of phase B of the stepper motor. I_{ph} illustrates the phase current of the stepper motor. I_1 presents the phase current of phase A and I_2 presents the phase current of phase B of the stepper motor. ω presents the rotor speed and θ is the rotos position. It can be seen in the generated waveforms that the phase voltages in phase A and B of the stepper motor are 90° displaced. In the same manner, the phase current in the phase A and B of the stepper motor are 90° displaced. The generated waveforms are alike sine waveforms. The generated phase voltage and phase current waveforms are in agreement with the theoretical equations. Moreover, it can be seen in the generated waveforms that the rotos position and rotos speed are well controlled. The control system could drive the implemented hybrid stepper motor with high precision, while executing a smooth and controlled angular rotation of the stepper motor's rotor. The simulation results show that the designed control system is capable of driving the hybrid stepper motor with desired working factors.

After the simulation of the designed control system, an experimental study was performed to evaluate the functionality of the developed system in generating the desired MFD, setting the position of the magnets, and measuring the generated MFD. Table 3 presents the test conditions and the results obtained from the experimental study. As presented in Table 3, during the experimental study, different amounts of MFD were set using the HMI unit of the AMMS. Afterwards, the system was run using the predetermined factors mentioned in Table 3. The implemented control system of the AMMS could calculate the distance between the magnets using Eq (1) and Eq (2) to achieve the desired MFD. Subsequently, the linear mechanisms are driven and the magnets are moved to the desired positions. The metrology unit of the AMMS measures the strength of the generated MF. The measured MFD is used as control feedback in the control system. In case there is a difference between the desired MFD and the measured MFD, the control system calculates the required linear repositioning and corrects the distance between the magnets to achieve the exact amount of desired MFD.

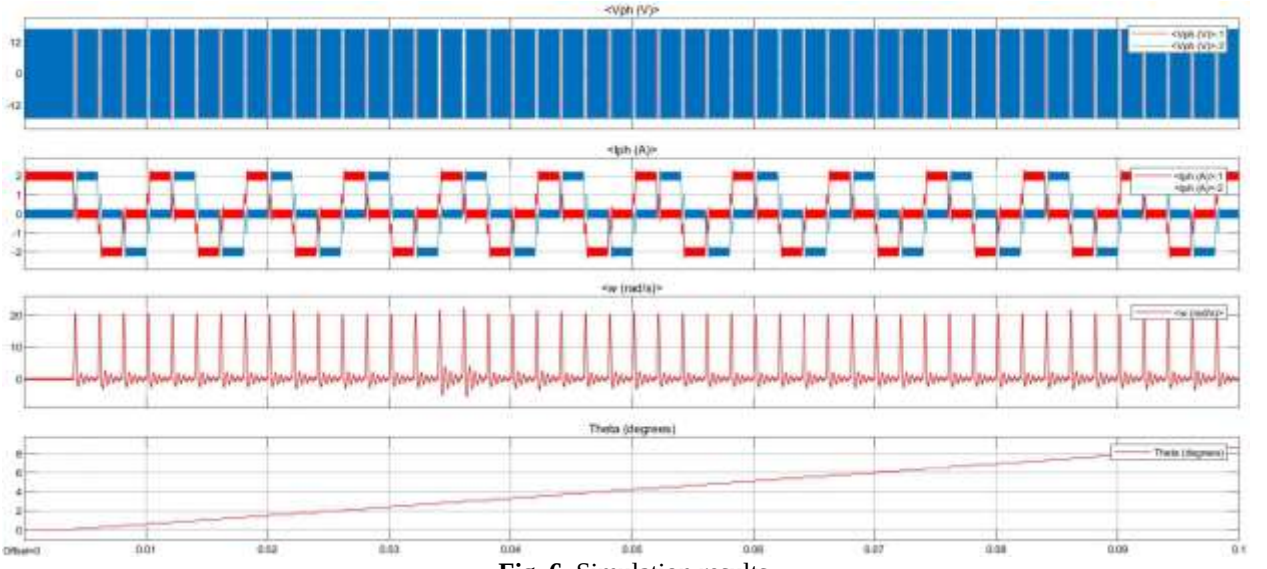

Fig. 6. Simulation results.

Table 3. The conditions of the experimental study and the obtained results.

Test	Repeat cycle	Desired MFD (T)	Calculated distance between magnets (mm)	Mean measured distance between magnets (mm)	Mean measured MFD before positioning correction (T)	Mean measured distance between magnets after correction (mm)	Mean measured MFD after positioning correction (T)
T1	5	0.10	48.2	48.22	0.098	48.09	0.102
T2	5	0.09	89.1	89.13	0.088	88.98	0.091
T3	5	0.08	94.5	94.51	0.076	94.18	0.078
T4	5	0.07	100.7	100.77	0.068	100.66	0.071
T5	5	0.06	109.1	109.13	0.064	109.28	0.062
T6	5	0.05	120.0	120.03	0.052	120.14	0.051
T7	5	0.04	129.4	129.41	0.043	129.63	0.042
T8	5	0.03	163.3	163.33	0.035	163.80	0.033
T9	5	0.02	172.7	172.72	0.023	173.40	0.021

The obtained results show that the control system is capable of calculating the distance between the magnets to achieve the desired MFD at the cutting zone with high accuracy. The on-machine metrology system for measuring the generated MFD, as well as the closed-loop control system, enables in-process measurement of the generated MFD and correcting the erroring in generated MFD when required. Figure 7 presents the generated graph using the obtained positioning results. The generated graph shows the distance between the magnets before and after the positioning correction.

The control system is capable of driving the linear mechanism with a positioning accuracy of 0.01 mm (10 µm), and mean linear positioning error less than 100 µm. The developed AMMS is capable of generating the desired MFD with a precision of 0.01 T in producing the desired MFD. The device could precisely set the distance between the magnets to achieve the desired MFD around the cutting zone with high-precision. Moreover, in a hybrid SPDT, the developed system could transmit the acquired data to the hybrid controller for further analysis. The application of AMMS could reduce the passive vibrations and positively influence the thermal conductivity of the workpiece material. The developed technique could enable generating a precise and controlled MF with desired MFD. Therefore, the developed method could be used in hybrid SPDT platforms for improving the machining conditions as well as the outcome of the SPDT process in terms of surface roughness.

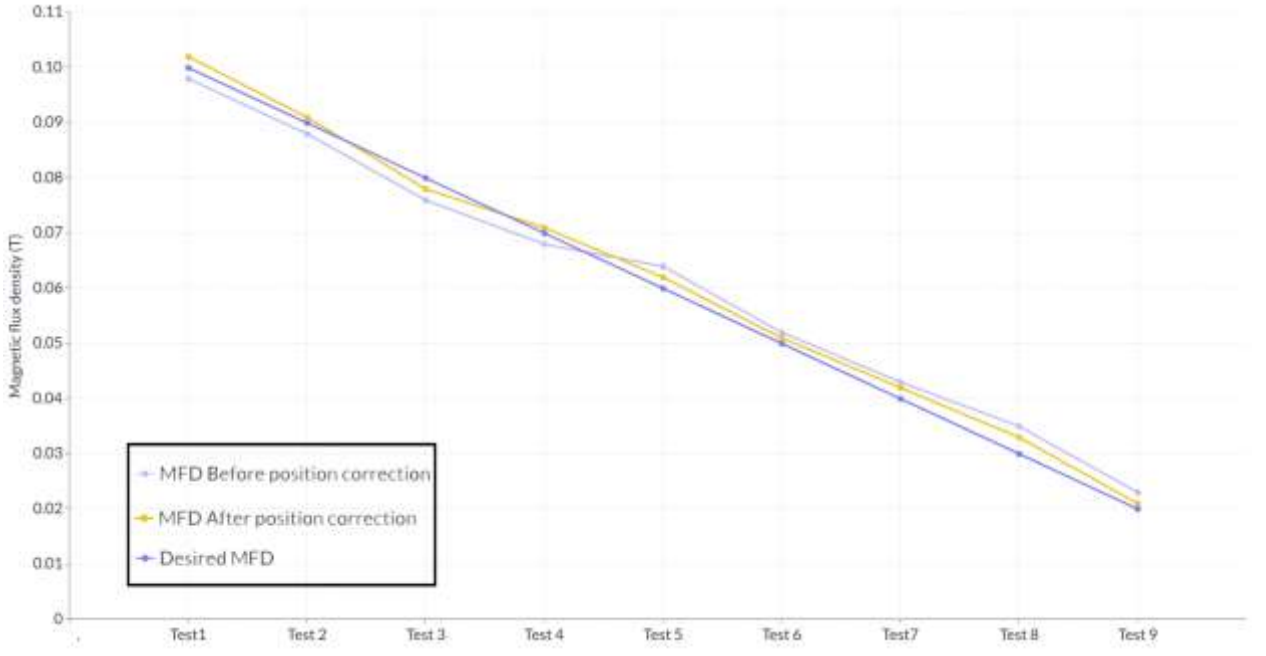

Fig. 7. The graphs generated from the obtained results of the generated MFD.

.

4. CONCLUSIONS

The SPDT technology is the state-of-the-are machining technique for advanced manufacturing of optical components with the minimum optical surface roughness and maximum surface accuracy. The application of hybrid SPDT technologies, by using different non-conventional machining techniques during the SPDT process, has been recently emerged. MF assistance is a low-cost passive technique that can significantly improve the machining conditions, including the thermal conductivity of the workpiece material and the passive vibrations of the machine tool. The proposed AMMS can generate a controlled MF with the desired MFD around the cutting zone. In addition, the AMMS has a precise on-machine metrology system for real-time measurement of the generated MFD. The results of modeling and experimental study justify the functionality of the developed system to be used in hybrid SPDT applications.

In a non-conventional/hybrid SPDT process, the developed AMMS could be used as a part of the hybrid machining technologies for applying a controlled MF around the cutting zone with desired MFD. In a hybrid SPDT process, the developed AMMS could communicate with main hybrid controller and transmit the acquired data including the measured MFD. This could enable on-machine metrology of the generated MFD with high precision, during the SPDT process. It is possible to set and modify the desired MFD before and during the manufacturing process using a hybrid controller and the HMI unit of the AMMS.

5. FUTURE WORKS

In the future experimental studies, the developed system could be used in non-conventional and hybrid SPDT platforms for on-machine measurement of MFD during the SPDT process. By using AMMS, the effect of the strength of MF on the machining factors could be determined. By using the AMMS in ultra-high-precision SPDT of engineering materials, the optimum MFD in different machining conditions, could be determined.

ACKNOWLEDGMENT

The authors would like to thank the office of Research Development of Nelson Mandela University for their support of this research.

REFERENCES

[1] Balasubramaniam, R., R.V. Sarepaka, and S. Subbiah, *Diamond turn machining: Theory and practice*. 2017: CRC Press.

[2] Hatefi, S. and K. Abou-El-Hossein, **"Review of single-point diamond turning process in terms of ultra-precision optical surface roughness".** T*he International Journal of Advanced Manufacturing Technology*, 2020. **106**(5): p. 2167-2187.

[3] Gupta, K., *Advanced Manufacturing Technologies*. 2017: Springer.

[4] Hatefi, S. and K. Abou-El-Hossein, **"Review of magnetic-assisted single-point diamond turning for ultra-high-precision optical component manufacturing".** *The International Journal of*

Advanced Manufacturing Technology, 2022. **120**(3): p. 1591-1607.

[5] Chavoshi, S.Z. and X. Luo, **"Hybrid micro-machining processes: A review".** *Precision Engineering*, 2015. **41**: p. 1-23.

[6] Li, Z., et al., **"Review of diamond-cutting ferrous metals"**. *The International Journal of Advanced Manufacturing Technology*, 2013. **68**(5-8): p. 1717-1731.

[7] Hatefi, S. and K. Abou-El-Hossein, "**Review of hybrid methods and advanced technologies for in-process metrology in ultra-high-precision single-point diamond turning"**. *The International Journal of Advanced Manufacturing Technology*, 2020. **111**(1): p. 427-447.

[8] Hatefi, S. and K. Abou-El-Hossein, **"Review of non-conventional technologies for assisting ultra-precision single-point diamond turning".** *The International Journal of Advanced Manufacturing Technology*, 2020. **111**(9): p. 2667-2685.

[9] Bhowmik, S. and D. Zindani, **"Overview of Hybrid Micro-manufacturing Processes"**, in *Hybrid Micro-Machining Processes*. 2019, Springer. p. 1-12.

[10] Lauwers, B., et al., **"Hybrid processes in manufacturing"**. *CIRP Annals*, 2014. **63**(2): p. 561-583.

[11] Peruri, S.R. and P.K. Chaganti, "**A review of magnetic-assisted machining processes"**. *Journal of the Brazilian Society of Mechanical Sciences and Engineering*, 2019. **41**(10): p. 450.

[12] Philip, J., P. Shima, and B. Raj, **"Enhancement of thermal conductivity in magnetite based nanofluid due to chainlike structures***". Applied physics letters*, 2007. **91**(20): p. 203108.

[13] Philip, J., P. Shima, and B. Raj**," Evidence for enhanced thermal conduction through percolating structures in nanofluids".** *Nanotechnology*, 2008. **19**(30): p. 305706.

[14] Yeo, S., M. Murali, and H. Cheah, **"Magnetic field assisted micro electro-discharge machining".** *Journal of Micromechanics and Microengineering*, 2004. **14**(11): p. 1526.

[15] Sodano, H.A. and J.-S. Bae, **"Eddy current damping in structures".** *Shock and Vibration Digest*, 2004. **36**(6): p. 469.

[16] Sodano, H.A., et al., "**Improved concept and model of eddy current damper"**. *Journal of Vibration and Acoustics*, 2006. **128**(3): p. 294-302.

[17] Liu, C., K. Jiang, and Y. Zhang, **"Design and use of an eddy current retarder in an automobile".** *International Journal of Automotive Technology*, 2011. **12**(4): p. 611-616.

[18] Hatefi, S. and K. Abou-El-Hossein, **"Feasibility Study on Design and Development of a Hybrid Controller for Ultra-Precision Single-Point Diamond Turning"**. *Majlesi Journal of Electrical Engineering*, 2019. **13**(2): p. 121-128.

[19] Hatefi, S. and K. Abou-El-Hossein, **"Design and Development of High-Precision Hybrid Controller for Ultra-Precision Non-Conventional Single-Point Diamond Turning Processes".** *Majlesi Journal of Electrical Engineering*, 2020. **14**(2): p. 61-70.

[20] Hatefi, S., O. Ghahraei, and B. Bahraminejad, **"Design and Development of a Novel Multi-Axis Automatic Controller for Improving Accuracy in CNC Applications"**. *Majlesi Journal of Electrical Engineering*, 2017. **11**(1): p. 19.

[21] Hatefi, S., O. Ghahraei, and B. Bahraminejad, **"Design and Development of a Novel CNC Controller for Improving Machining Speed".** *Majlesi Journal of Electrical Engineering*, 2016. **10**(1).

[22] Coey, J.M.D., *Rare-earth iron permanent magnets*. 1996: Oxford University Press.

[23] Bendjedia, M., et al., **"Position control of a sensorless stepper motor"**. *IEEE Transactions on Power Electronics*, 2012. **27**(2): p. 578-587.